Exoplanet Characterisation Observatory (EChO)

Assessment Phase Payload Study

Planet Formation & EChO

ECHO-TN-YYYY-ZZZ

Issue XX

Prepared by: Richard Nelson (QMUL), Diego Turrini (INAF), Mauro Barbieri (INAF) Date:

Checked / Approved by: Date:

DOCUMENT CHANGE DETAILS

Issue	Date	Page	Description Of Change	Comment

EChO Origins Technical Note

Exoplanetary atmospheres and their link to planetary history

The primary objective of the EChO mission is to accurately measure transmission spectra for extrasolar planets during primary transits, and day-side spectra from secondary eclipses. The operating wavelength range (1 – 11 μm or 1 – 16 μm, depending on the final configuration) covers key absorption signatures from the molecular species CH_4, H_2O, CO_2 and CO, whose relative strengths scale with the abundances present in the planetary atmosphere. Chemical modelling shows that these abundances are particularly sensitive to the heavy-element content of the atmosphere (measured through the C/H and O/H ratios), and the C/O ratio (see Moses et al 2013, for example). Determination of the atmospheric elemental abundances from the measured spectra will provide important constraints on the formation, migration and enrichment history of the observed extrasolar planets.

Spectroscopic observations of extrasolar planets using HST and Spitzer have already confirmed the existence of various elements and molecules such as sodium, water, methane, and carbon dioxide in the atmospheres of hot-Jupiters (e.g. Tinetti et al. 2007; Swain et al. 2009). Recent observations of the transiting hot-Jupiter Wasp-12b suggest an atmosphere abundant in CO and deficient in H_2O, consistent with an atmospheric C/O ratio > 1, in contrast to the solar value C/O=0.54 (Madhusudhan et al. 2011). Analysis of transmission and day-side spectra for the transiting 6.5 M_{Earth} super-Earth GJ 1214b suggest a metal-rich atmosphere (e.g Bean et al. 2011), in agreement with the general expectation that low mass planets will be well-endowed with heavy elements. A similar conclusion has been reached for the hot-Neptune GJ 436b, whose day-side spectrum lacks a clear signature of CH_4 while displaying abundant CO and CO_2 (Madhusudhan & Seager 2011). The derived carbon chemistry mixing ratios are consistent with chemical models that assume a heavy element abundance enhanced above solar by a factor > 50 (Moses et al 2013). Although these and other data pertaining to extrasolar planet atmospheres are tantalising, uncertainties originating in the relatively low signal to noise, and low spectral resolution, mean that definitive conclusions concerning atmospheric abundances cannot be made. These data are not accurate enough to discriminate between different formation and migration scenarios for the observed planets. The spectral resolution and signal-noise to be achieved by EChO will dramatically improve the situation and allow atmospheric compositions to be measured with unparalleled accuracy. Combining these data with estimates of planetary bulk compositions from accurate measurements of their radii and masses will allow degeneracies associated with planetary interior modelling to be broken (e.g. Adams et al 2008), giving unique insight into the interior structure and elemental abundances of these alien worlds.

The original view of the set of events and mechanisms involved in planetary formation was derived from observations of the Solar System as it is today. The original assumption was that planetary formation is a local, orderly process that produces regular, well-spaced and, above all, stable planetary systems and orbital configurations. However, with the discovery of increasing numbers of extrasolar planetary systems through ground- and space-based observations, it has become evident that planetary formation can result in a wide range of outcomes, most of them not obviously consistent with the picture derived from the observations of the Solar System.

The orbital structure of the majority of the discovered planetary systems seems to be strongly affected by planetary migration. This can arise through the exchange of angular momentum with the

circumstellar disk in which the forming planets are embedded (see e.g. Papaloizou et al 2007, Chambers 2010 and references therein), and through the so-called "Jumping Jupiters" mechanism (Weideschilling & Marzari 1996; Marzari & Weidenschilling 2002), which invokes multiple planetary encounters with a chaotic exchange of angular momentum and energy between the bodies involved. Each of these migration mechanisms will have different implications for the chemical make-up of the planetary atmosphere, as migration through a disc allows the planet to accrete from regions with varying chemical abundances. This is not true for hot Jupiter formation through planetary scattering.

The growing body of evidence that dynamical and collisional processes, often chaotic and violent, can dramatically influence the evolution of young planetary systems gave rise to the idea that our Solar System could have undergone the same kind of evolution and represent a "lucky" case in which the end result was a stable and regular planetary system. As we will discuss shortly, different attempts at modelling have been performed on this regard, but in the context of EChO the underlying and important idea is that processes shaping the formation and evolution of planetary systems are general. As a consequence, there are lessons that can be drawn from the Solar System and used to shed light on the link between the history of a planetary system and the atmospheric composition of its giant planets.

The timeline of planetary systems

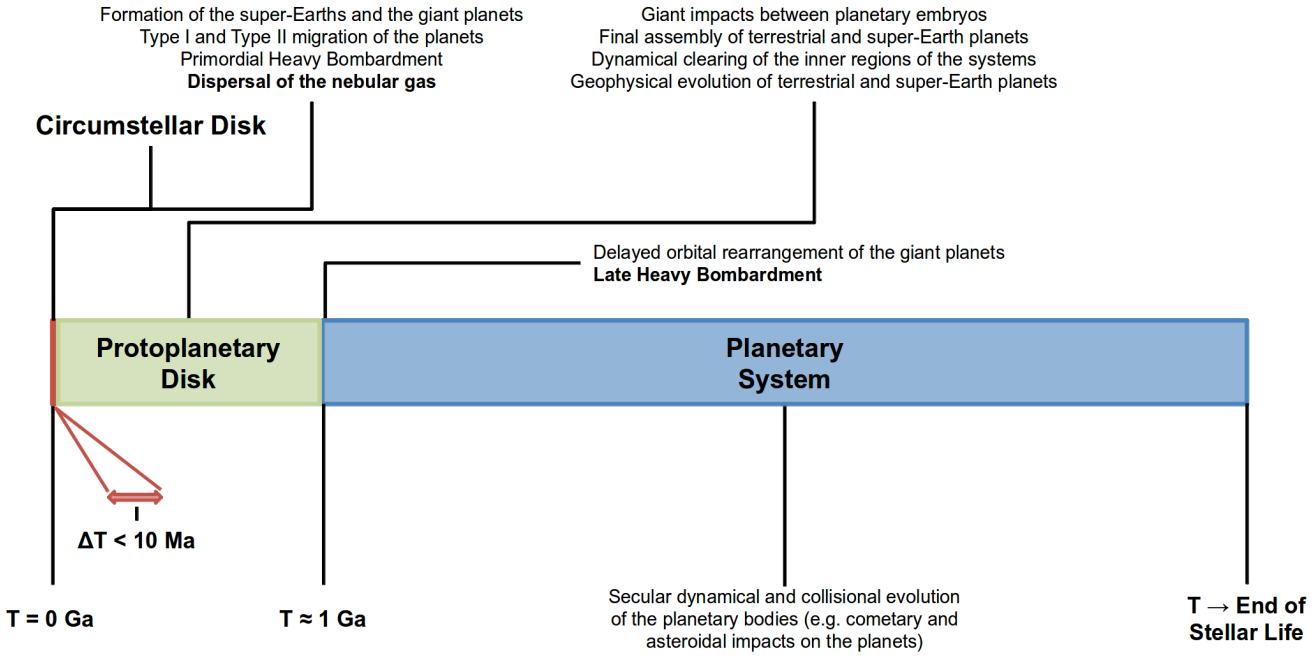

[Following the introduction, we present the generalized timeline of the evolution of planetary systems, based on what we know from the Solar System. We use the timeline to briefly introduce the major events taking place across the history of all planetary systems and introducing the effects (that will be developed in more detail in the following subsections) for the composition of the atmospheres of the planets (focusing on the role of giant planets). In order to emphasize the clarity, in this part of the section we proceed time-wise, while in the subsections we proceed process-wise.]

Planetary formation and composition

EChO will target super-Earths, Neptune-like and Jupiter-like exoplanets on relatively short period orbits. These broad classes of planets are all expected to have very different formation and migration histories that will be imprinted on their atmospheric and bulk chemical signatures. Within each of these planet taxonomic classes, the stochastic nature of planetary formation will be reflected in significant variations in the measured abundances, providing important information about the diverse formation and migration pathways experienced by planets are members of the same broad class. Reconstructing formation histories from spectral measurements presents a challenging inversion problem, but can nonetheless provide very useful constraints, as we detail below.

Formation processes and migration influence a planet's composition in numerous ways. For example, we clearly expect gas giant planet formation via gravitational instability to result in very different bulk compositions and atmospheric abundances compared with planets that form through core accretion. In general one may expect planets formed via the former process to reflect the bulk composition of the nascent protoplanetary disc, whereas plants formed through core accretion can display a range of abundance ratios that depend on the relative accretion rates for planetesimals and gas. Gas giant planets are expected to have atmospheric compositions very different from the presumably heavy element-rich atmospheres of super-Earths, if the examples of Uranus and Neptune in our Solar System provide a useful guide. Very little research has been done on this important question, mainly because the large uncertainties in current measurements of elemental abundances provide little in the way of discrimination between different models and scenarios. EChO will change this, stimulating in-depth analyses of the link between formation, migration, and post-formation enrichment. In the absence of existing detailed model results, we outline a number of different simplified formation and migration scenarios to illustrate how diverse atmospheric elemental abundances can arise.

Formation of gas giants through gravitational instability during the earliest phases of a protoplanetary disc's evolution will lead initially to atmospheric abundances that are essentially the same as the central star's. Recent studies show that rapid inward migration of planets formed in this way occurs on time scales ~ 10^3 yr (e.g. Baruteau et al 2011, Zhu et al 2012), too short for significant dust growth or planetesimal formation to arise between formation and significant migration occurring. As such, migration and accompanying gas accretion should maintain the initial planetary abundances. As we describe later, post-formation enrichment may occur through bombardment from neighbouring planetesimals or long-period star-grazing comets, but this enrichment will likely occur in an atmosphere with abundances that are essentially equal to the stellar values.

In its simplest form, the core accretion model of planet formation begins with the growth and settling of dust grains, followed by the formation of planetesimals that accrete to form a planetary core. Growth of the core to a mass in excess of a few Earth masses allows settling of a significant gaseous atmosphere from the surrounding nebula. Halting growth at this point results in a super-Earth or Neptune-like planet. Continued growth through accretion of planetesimals and gas can lead to runaway gas accretion, forming a Jupiter-like gas giant. A key issue for determining the atmospheric abundances of a forming planet is the presence of ice-lines at various distances from the central star, where volatiles such as water, carbon dioxide and carbon monoxide freeze-out onto grains and are incorporated into planetesimals. Considering a typical protoplanetary disc orbiting a solar-type star, figure 1 shows that a H_2O ice-line is expected at ~2 au, a CO_2 ice-line at ~10 au, and a CO ice-line at ~ 40 au. The

atmospheric abundances of a planet during formation will therefore depend on where it forms and the ratio of gas to solids accreted at late times. We recall that EChO will study planets with relatively short orbital periods, and these must have undergone large scale migration during their evolution: the inner regions of protoplanetary discs contain too little solid material for *in situ* formation of planetary systems similar to those discovered by the Kepler mission (e.g. Kepler 11, Lissauer et al 2011) and radial velocity surveys (e.g. Gliese 581, Mayor et al 2009). The final C/O ratio of the planet will therefore depend on how it accretes as it migrates through the disc.

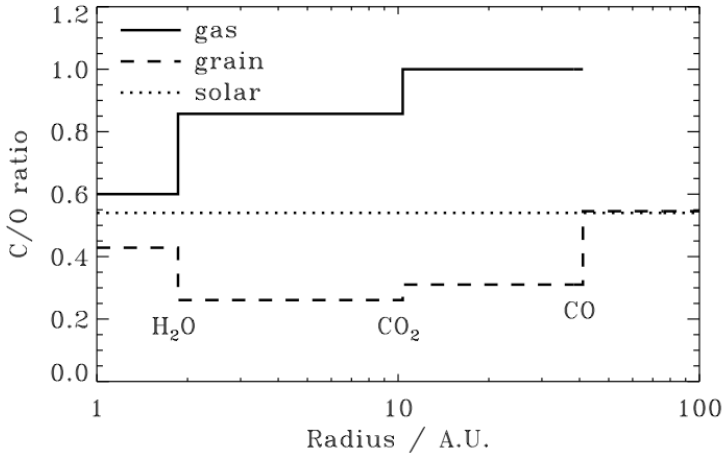

Figure 1: Locations of the ice-lines and their influence on the C/O ratios for the gas and solids (adapted from Oberg et al 2011)

For the purpose of illustration, we now consider a number of highly simplified planetary accretion and migration scenarios and their influence on the atmospheric C/O ratio. The protoplanetary disc is assumed to be of solar abundance, giving rise to an overall C/O ratio ~ 0.54, as shown in figure 1. Interior to the H_2O ice-line, carbon- and silicate-rich grains are condensed, leading to an increase of the gas-phase C/O ~ 0.6 (due to the slight overabundance of oxygen relative to carbon in these refractory species). Water condenses between the H_2O and CO_2 ice-lines, increasing the gas-phase C/O ~ 0.85 through removal of oxygen into the frozen-out H_2O, and decreasing the solid phase C/O ~ 0.26. Between the CO_2 and CO ice-lines the CO_2 freezes out, increasing the gas phase C/O ~1 and moderately increasing the solid phase C/O ratio ~ 0.31. Various formation scenarios for gas giant planets are now assumed, based on figure 1, and their implications for the atmospheric C/O value are calculated.

Scenario 1: A solid core forms at 5 au, migrates inward and only starts to accrete gas once it has moved interior to the H_2O ice-line. Gas accretion is not accompanied by any accretion of solids, leading to an atmospheric C/O ratio ~ 0.6.

Scenario 2: This is identical to scenario 1, except that gas accretion interior to the H_2O ice-line is accompanied by accretion of solids such that the C and O abundances of the accreted material equals the solar value. The atmospheric C/O ratio is ~ 0.54.

Scenario 3: A solid core forms at 5 au and accretes gas exterior to the H_2O ice-line while migrating inward, without accreting any solids. Before crossing the H_2O ice-line the planet opens a deep gap that

prevents further accretion. The planet continues to migrate inward. The final C/O ratio is ~ 0.86.

Scenario 4: A solid core forms at 15 au and accretes gas but no further solids from beyond the CO_2 ice-line before forming a deep gap that prevents further gas accretion. The planet migrates inward to form a hot Jupiter and the final atmospheric C/O ratio is ~ 1.

Scenario 5: A solid core forms at 15 au, migrates inward, and accretes equal amounts of gas from the region outside the CO_2 ice-line, the region between the H_2O and CO_2 ice-lines, and the region interior the H_2O ice-line. No solids are accreted. The final atmospheric C/O ratio is ~ 0.77.

Scenario 6: A solid core forms at 15 au, migrates inward and accretes gas as in scenario 5, but also accretes 10% of its atmosphere in the form of solids as it migrates. The final atmospheric C/O ratio is ~ 0.73.

All of the above scenarios assume gas-dominated accretion and lead to solar or super-solar atmosphere C/O ratios because of the tendency of O-rich compounds to freeze-out at higher temperatures. Sub-solar values of the C/O ratio can be obtained through substantial accretion of silicate-rich planetesimals as the planet migrates interior to the H_2O ice-line. These examples simply serve to illustrate that a variety of formation, migration and accretion scenarios can lead to a broad distribution of C/O ratios. The final C/O value correlates with where and how the planet forms and migrates in a predictable manner, but this final value is not unique for all scenarios. Detailed predictions of the expected diversity of C/O ratios in planetary atmospheres require planetary formation models to be computed that account for the evolving chemistry of the protoplanetary disc and the chemical abundances of the accreted material.

Finally, we note that gas disc-driven migration is only one plausible mechanism by which planets may migrate. As discussed above, the large eccentricities (and obliquities) of the extrasolar planet population suggest that planet-planet gravitational scattering ("Jumping Jupiters") may be important (e.g. Weideschilling & Marzari 1996; Marzari & Weidenschilling 2002; Chatterjee et al 2008), and this is likely to occur toward the end of the gas disc lifetime when its ability to damp orbital eccentricities is diminished. When combined with tidal interaction with the central star, planet-planet scattering onto highly eccentric orbits can form short-period planets that have not migrated toward the central star while accreting from the protoplanetary disc. These planets are likely to show chemical signatures that reflect this alternative formation history, being composed of higher volatile fractions if they form exterior to the H_2O ice-line.

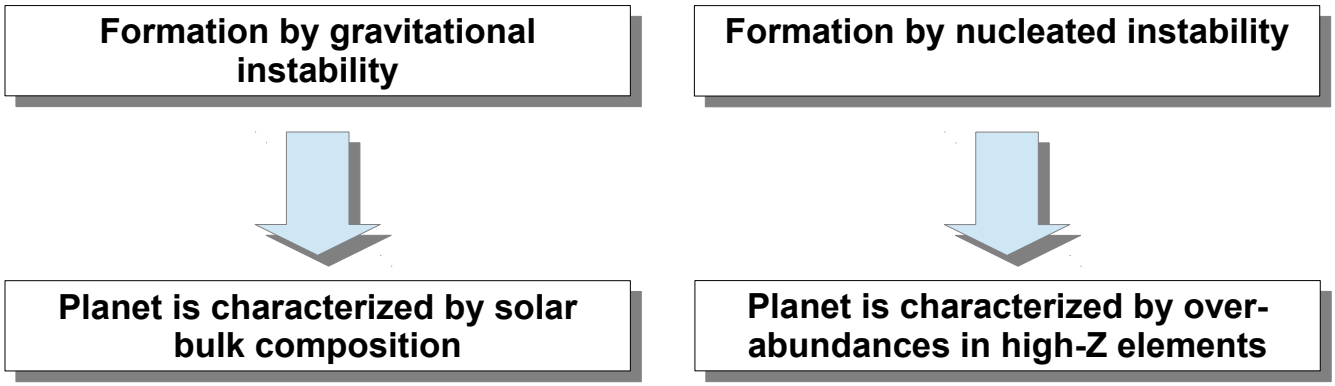

Post-formation evolution, late accretion and protoplanetary disks

When they form, giant planets trigger a phase of intense bombardment and remixing of solid material in the protoplanetary disk in which they are embedded (Safronov 1969; Weidenschilling 1975; Weidenschilling et al. 2001; Turrini et al. 2011, 2012; Coradini et al. 2011). In the Solar System this event has been named the Jovian Early Bombardment (Turrini et al. 2011, 2012; Coradini et al. 2011) as Jupiter was likely the first planet to form (Safronov 1969; Coradini et al. 2011). As a new phase of bombardment and remixing, likely of decreasing intensity, will be triggered by the formation of each giant planet in a planetary system hosting more than one, a more general name for this class of events is the Primordial Heavy Bombardments (Coradini et al. 2011).

The duration of the phase of bombardment and remixing triggered by the formation of Jupiter in the Solar System was estimated to be of about 0.5-1 Ma (Weidenschilling 1975; Turrini et al. 2011, 2012). The bombardment is caused by the interplay between the gravitational scattering of planetesimals near-by the newly formed giant planet and the appearance of the orbital resonances in regions farther away (Safronov 1969; Weidenschilling 1975; Weidenschilling et al. 2001; Turrini et al. 2011, 2012).

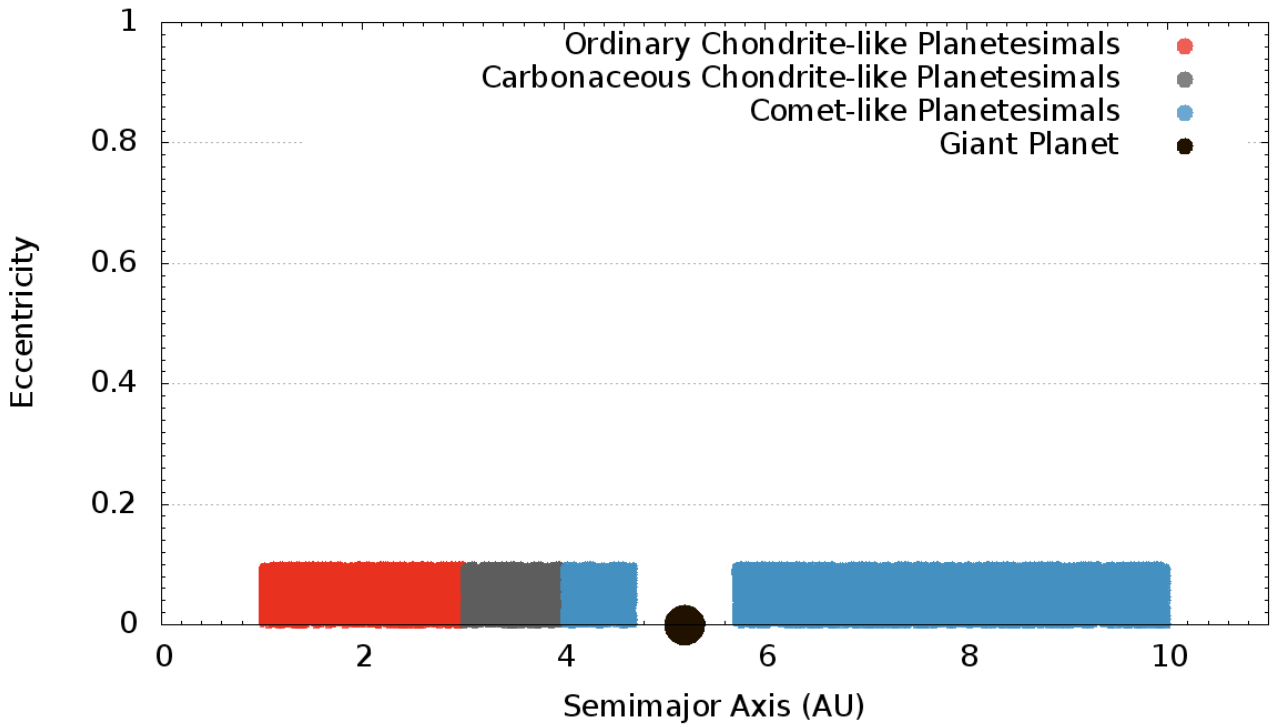

Figure 2: Protoplanetary disk and embedded giant planet at the beginning of the simulations for the late accretion of giant planets. The massless particles have been divided into compositional classes according to their semimajor axes. The Snow Line is assumed at 4 AU. The initial number of massless particles is 20000.

From the point of view of EChO, one of the main effects of this class of events is the reshuffling of the solid material present in the protoplanetary disks: volatile-rich objects from beyond the Snow Line are injected into the inner, volatile-depleted regions of the disk while rocky, metal-rich bodies are transferred from the latter to the former. The net effect is a change in the rock-ice and metal-ice ratios in the different regions of the protoplanetary disks. During this phase of remixing, the orbital regions of the giant planets are crossed by these fluxes of planetesimals and a fraction of the migrating material is captured by the giant planets themselves, thus enriching their atmospheric composition in high-Z elements.

To illustrate the effects of these events and the implications for the interpretation of the observations by the EChO mission, we will take advantage of the following toy model. We consider a Jupiter-sized giant planet disk embedded into a disk of massless particles representing the protoplanetary disk. Dynamical friction between the bodies populating the protoplanetary disk and the effects of gas drag are ignored for simplicity. The giant planet (see Fig. 2) is initially on a planar (i=0°) and circular (e=0) orbit with the semimajor axis of Jupiter (a=5.2 AU). The massless particles (see Fig. 2) are distributed between 1 AU and 10 AU, leaving empty the region between 4.7 AU and 5.7 AU to simulate the gap created by the formation of the giant planet. The massless particles initially have eccentricities randomly distributed between 0 and 0.1 (Weidenschilling 2008) and inclinations randomly distributed between 0° and 1.7° (Turrini et al. 2011). The Snow Line is assumed at 4.0 AU and the massless

particles are divided into compositional classes according to their semimajor axes. Using the Solar System as a template, bodies inside 3 AU are considered composed of a mixture of rocks and metals analogous to ordinary chondrites. Bodies in the region between 3.0 AU and 4.0 AU are assumed transitional bodies depleted in metallic iron (most iron is in oxydized form) and enriched in carbon and water similarly to the carbonaceous chondrites. Finally, bodies from beyond 4.0 AU are assumed to be volatile-rich bodies similar to the comets.

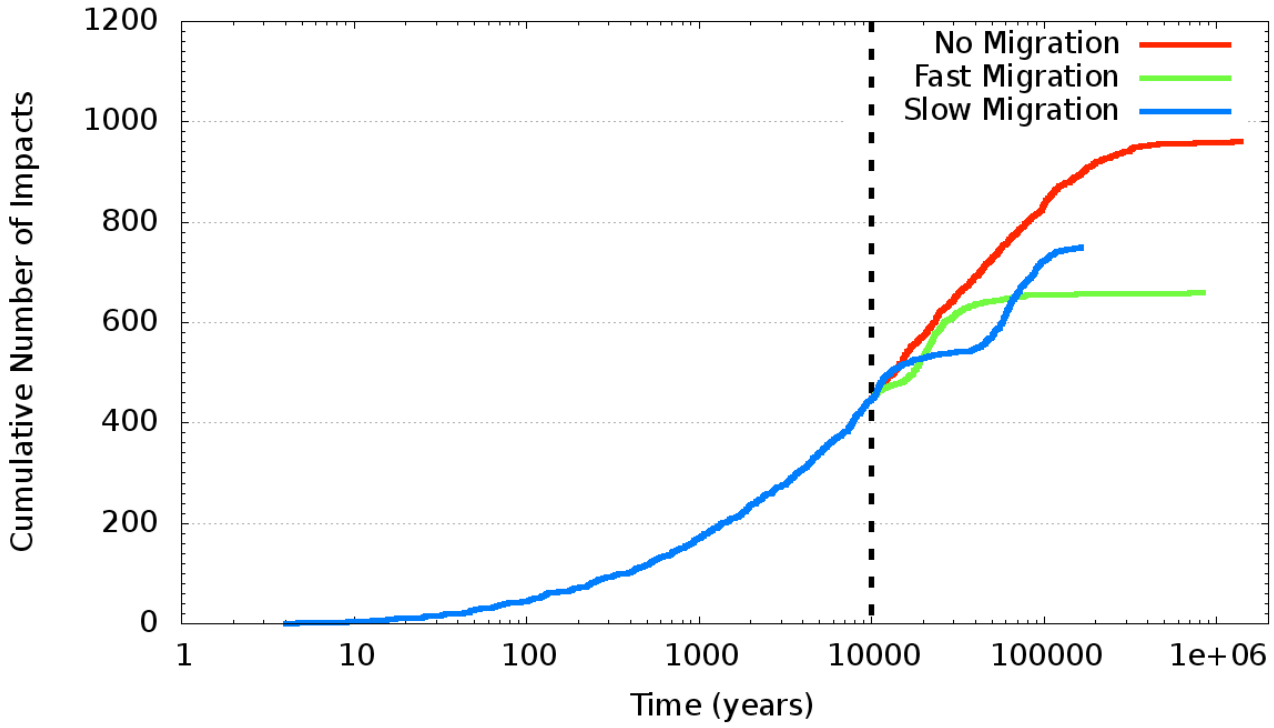

Figure 3: Number of impacts on the giant planet as a function of time in the three scenarios considered. The vertical dashed line marks the beginning of the planetary migration in those scenario where it is present. The initial number of massless particles is 20000.

We consider three scenarios: the giant planet not migrating (i.e. standing on its initial orbit, hereafter labelled as the *no migration* case), the giant planet migrating to a semimajor axis of 0.7 AU with an e-folding time of 5×10^3 years (i.e. 99.4% of the migration is completed in 2.5×10^4 years, hereafter labelled as the *fast migration* case) and the giant planet migrating to a semimajor axis of 0.7 AU with an e-folding time of 3×10^4 years (i.e. 99.4% of the migration is completed in 1.5×10^5 years, hereafter labelled as the *slow migration* case). Migration, when present, always starts after 10^4 years from the beginning of the simulations. The migration scheme is implemented following Hahn & Malhotra (2005). As shown in Fig. 3, about 33% to 50% of the impacting particles are accreted by the giant planet extremely quickly in the first 10^4 years. Then, if the giant planet migrates, the late accretion phase slows down significantly for the first 2 e-folding times (i.e. the faster part of the migration, while the giant planet complete about 86% of its displacement). Accretion starts again across the next 3 e-folding times (i.e. the slowest part of the migration, while the giant planet complete about 13% of its displacement). If the giant planet does not migrate, the late accretion extends over about 5×10^5 years.

Accretion in the no migration case is the most efficient, with the giant planet capturing about 4.8% of the solid material in the protoplanetary disk. The slow migration is more efficient accretion-wise than the fast migration case, with 3.8% vs 3.3% of the solid material of the disk captured by the giant planet. Assuming the disk is analogous to the Minimum Mass Solar Nebula and has a surface density profile governed by the relationship $\sigma = 2700\ r^{-3/2}$ g cm^{-2} (Coradini et al. 1981) where r is the orbital distance in AU, the mass of the disk we considered would be about 27.5 $M_\oplus$. Assuming that the giant planet had a core of 5 $M_\oplus$, this leave a total of 22.5 MÅ in the massless particles. The accreted masses would then translate in 1.1 $M_\oplus$ (no migration scenario), 0.86 $M_\oplus$ (slow migration scenario) and 0.75 $M_\oplus$ (fast migration scenario).

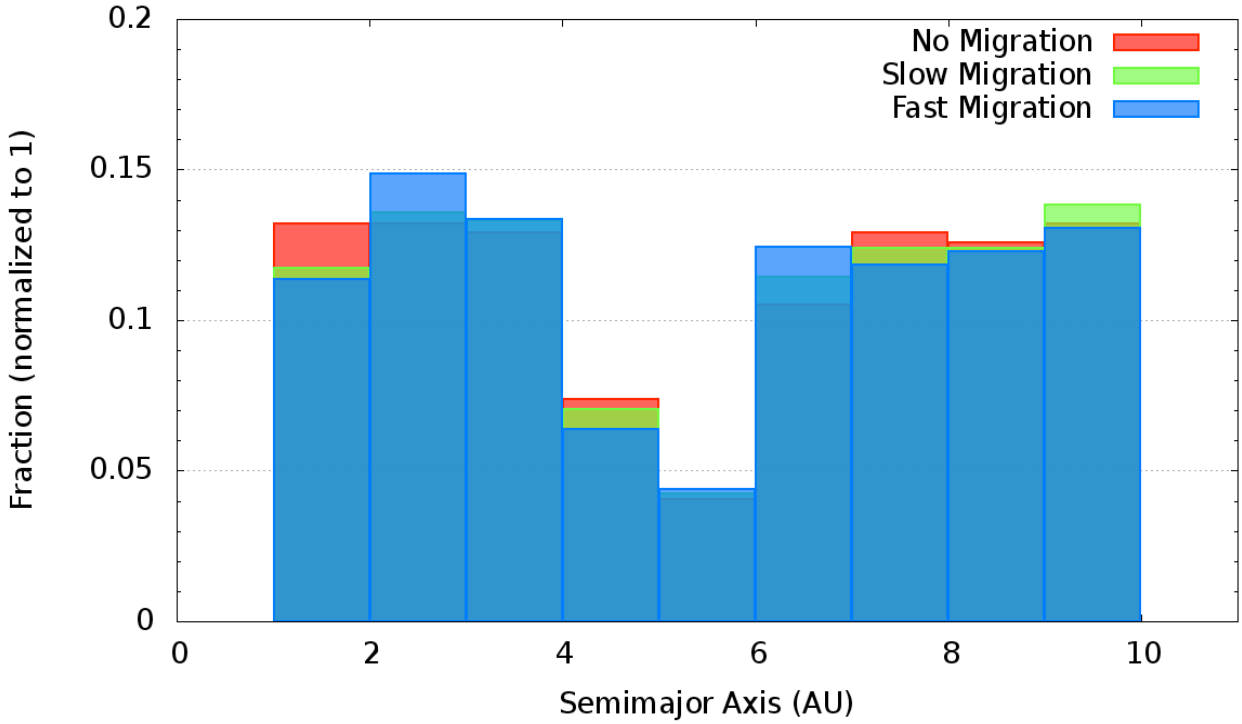

Figure 4: Fractions of the capture particles coming from the different regions of the disk of massless particles (red for the no migration scenario, green and blue for the fast and slow migration scenarios respectively).

As the dynamical and physical model underlying this toy model is quite simplistic, these numbers should be regarded just as more detailed back-of-the-envelope calculations. Yet, they provide a first indication of the effects of the post-formation accretion. While the overall accretion efficiency varies between the three scenarios, Fig. 3 shows that the relative importance of the different source regions in the protoplanetary disk varies little. This means that a newly formed giant planet can quickly accrete solid material from a vast feeding zone characterized by different compositions of the planetesimals. About 40% of the accreted bodies originate from the inner (1 - 4 AU) region of the protoplanetary disk.

If we use water and the most abundant elements (Si, C, N, S, Fe) as tracers of the composition of the accreted bodies, bodies originating between 1 - 3 AU would be composed by 30% Fe and 70% Si (and

possibly also by S). Bodies coming from the 3 - 4 AU transition region would be composed by 1% Fe, 85% Si, 5% C, 9% H2O. Finally, bodies originating beyond the Snow line (4 - 10 AU) would be composed (on average) by 72.8% H2O, 25.84% C, 0.62% N, 0.74% S. Because of the condensation sequence of the different elements and chemical species in the protoplanetary disk (Lewis 2004), therefore, the post-formation accretion phase would bring to the giant planet high-Z materials with relative abundances of the different elements that are highly non-solar. As a consequence, the effects of this process should reflect into the C/O, S/O, N/O ratios and (possibly) in the content of silicates and metals in the atmospheres of the giant planets. Metals and silicates, however, had been observed by the Galileo spacecraft after the impact of the comet Shoemaker-Levy 9 on Jupiter only for a limited time (Taylor et al. 2004), which could imply that they are removed efficiently (i.e. in a matter of months) from the observable regions of the atmosphere of a giant planet in contrast, to water, for example (see also Sect. “Secular contamination of planetary atmospheres”).

As mentioned above, the reshuffling process started by the Primordial Heavy Bombardment has a duration of about 1 Ma. At its end, however, it transitions into a longer phase of reshuffling where the planetary embryos in the protoplanetary disk scatter planetesimals inside the now-depleted locations of the orbital resonances with the giant planets. This phase has been studied, in the Solar System, to investigate the mass depletion of the asteroid belt (Wetherill 1992; Chambers & Wetherill 2001; Petit et al. 2001; O'Brien et al. 2007). During this phase, the population of planetesimals in the affected regions decays exponentially, decreasing by about two orders of magnitude in about 100 Ma (see e.g. O'Brien et al. 2007). Across these 100 Ma the giant planets continues to capture part of the solid material that is expelled by the resonances: in principle, this process could possibly be even more efficient in the case of giant planets on inner orbits (e.g. less than 1 AU) if they did not completely dispersed the planetary bodies populating the regions they crossed while migrating.

Limited data are currently available on the implications of the phase of dynamical clearing for the composition of the giant planets taking into account the role of planetary embryos. The best estimate to date is the one done by Guillot & Gladman (2000), who assessed the capture efficiency of the four giant planets during the 100 Ma following the formation. The work of Guillot & Gladman (2000) was based on a simplified model similar to the toy model we used to illustrate the effects of the Primordial Bombardment. The disk of massless particles extended from 4 AU to 35 AU and planetary embryos were not included in the simulations. The cumulative capture efficiency of the four giant planets was found to be about 4%, i.e. of the same level as the one found with our toy model for Jupiter alone. It would therefore appear that the combined perturbations of the giant planets, once they are all present in the planetary system, and the effects of concurrent accretion make late accretion very inefficient after the first few Ma (ejection from the planetary system is favoured). This is confirmed also by Guillot & Gladman (2000), who in a second simulation show that the accretion efficiency of Jupiter alone could rise up to 7-8% in a disk extending between 4 AU and 13 AU, so twice as much as that of the four giant planets cumulatively (unluckily, the timescale over which this capture rate is achieved is not specified).

Extensive migration of the giant planets, both due to the interaction with the disk or to planet-planet scattering (i.e. the Jumping Jupiter mechanism, Weidenschilling & Marzari 1996; Marzari & Weidenschilling 2002) can supply an alternate evolutionary path to the previously described picture derived from the Solar System. The dynamical effects of the migrating planet on the protoplanetary disk would replace the slow erosion due to the interplay between planetary embryos and orbital resonances with the giant planets, but the end result would be analogous: the reshuffling of material

from different regions of the protoplanetary disk and the depletion of the population of planetesimals with a consequence capture of part of the removed population by the giant planets. As our toy model shows for a very simple configuration of the planetary system, the migrating giant planet would still capture material from a wide range of orbital distances. Another, more complex example is constituted by the so-called "Grand Tack" scenario (Walsh et al. 2011, 2012), where the four giant planets of the Solar System are suggested to migrated inward, then outward and get locked in a resonant configuration. During their extensive migration, the giant planets would scatter and redistributed the primordial planetesimals in the Solar System and likely capture a fraction of them. While it has been argued that this scenario has a low probability of reproducing the actual configuration of the Solar System (D'Angelo & Marzari 2012), the richness of orbital configurations of the known extrasolar planets can imply that several of the other planetary systems differing from our Solar System can be the outcome of the "failed" cases of this kind of evolutionary path. The results of Guillot & Gladman (2000) on the concurrent accretion and of our toy model for the accretion efficiency of migrating planets suggest, however, that in such a scenario the fraction of captured material (i.e. the late accretion) would be low.

A Jumping Jupiters evolution can also take place at a later time as has been hypothesized in the case of the Solar System by the so-called Nice Model (Gomes et al. 2005; Tsiganis et al. 2005; Morbidelli et al. 2005). The Nice Model is a Jumping Jupiter scenario formulated to link the event known as the Late Heavy Bombardment (Tera et al. 1974), assumed to have occurred about 600-800 Ma after the formation of the Solar System (see Fig. 1) to a migration event involving all the giant planets. In the Nice Model, the giant planets of the Solar System are postulated to have been initially located on a more compact orbital configuration than their present one and to interact with a massive primordial trans-neptunian region. The gravitational perturbations among the giant planets are initially mitigated by the trans-neptunian disk, whose population in turn is eroded. Once the trans-neptunian disk becomes unable to mitigate the effects of the interactions among the giant planets, the orbits of the latter become excited and a series of close encounters takes place. The end result of the Jumping Jupiters mechanism in the Nice Model is a small inward migration of Jupiter and marked outward migration of Saturn, Uranus and Neptune (Tsiganis et al. 2005). Due to the late time at which this migration and the associated bombardment take place and the depletion previously occurred in the population of planetesimals, however, the amount of solid material captured by the giant planets across the Late Heavy Bombardment would be quite limited. Matters et al. (2009) estimated that the accreted material would amount to 0.15 $M_\oplus$ for Jupiter, 0.08 $M_\oplus$ for Saturn and ~0.05 $M_\oplus$ for Uranus and Neptune. In the case of Jupiter, the material accreted during such a late event would be about an order of magnitude lower than the one accreted immediately after its formation.

These results collectively seem to indicate that the late accretion phase can in principle extend over a long temporal interval (500 Ma – 1 Ga) but that the magnitude of its effects decreases quickly with time, so that the main role is played by the first few Ma after the formation of a giant planet. Late accretion then turns into a slow, secular contamination process whose temporary effects, however, can have implications for the observation that EChO will perform and their interpretation, as will be illustrated in the next section.

Secular contamination of planetary atmospheres

Once they complete the most active and violent phases of their evolution, planetary systems enter a

stationary phase governed by secular processes. During this phase, the main processes affecting the atmospheric composition of the planets are impacts, atmospheric chemistry and, in the case of short-period planets, the stellar radiation and wind. Impacts, in particular, allow the transfer of material between different planetary bodies and between different orbital regions, continuing the remixing process that acts across the early phases of the evolution of planetary system but at a much lower rate. An example of this process in the Solar System is represented by the flux of comets impacting Jupiter, the most famous (and studied) of which is the impact of comet Shoemaker-Levy 9 (SL9 in the following) in 1994. Across the last 17 years the giant planet has been hit by five impactors: SL9 itself in 1994 (~5 km in diameter), then a sub-km impactor in 2009 (~10 m in diameter), two in 2010 (~500 m in diameter the first and undetermined the second) and one in 2012 (< 10 m in diameter). A sixth impact of a meteoroid was observed by Voyager 1 in 1979 (estimated mass of 11 kg, i.e. ~10 cm in diameter, Cook & Duxbury 1981). It must be stressed that these impact rates do not represent the real flux on Jupiter, but they are more likely a reflection of the observational coverage of the giant planet.

Recent results from the Herschel mission (Cavalié et al. 2013) indicate that the spatially-resolved distribution of stratospheric water for Jupiter cannot be explained by local processes or a steady state flux of interplanetary dust particles, and are instead a reflection of the impact of comet SL9. In particular, about 95% of the stratospheric water content of the giant planet as been reported to be due to this cometary impact. Similar but non-spatially resolved results were previously obtained for both water, CO and CO_2, supporting the case for an external source for these molecules as the thermal and pressure profiles in the atmosphere of Jupiter create a transport barrier between troposphere and stratosphere (see Cavalié et al. 2013 and reference therein), where water is expected to condense. The mixing ratio of stratospheric water modelled from the measurements of Herschel is 1.7×10^{-8} (Cavalié et al. 2013). In the framework of EChO, the fact that the persistence of water in the stratosphere to Jupiter is comparable with (or, as it seems, longer than) the expected duration of the mission and the maximum observational time-scale for the Ultra-Deep Survey mode is of particular importance, especially as the estimated mixing ratio is compatible with the observational capabilities of EChO.

To link the atmospheric composition of the exoplanets studied by EChO to their formation it is therefore mandatory to be able to discriminate the (plausibly) transient contribution in high-Z elements due to external sources from the constant one due to the bulk composition of the planet. To get a zero-order estimate of the implications of secular, cometary impacts for the observations of EchO we can use a simple toy model. We consider the planet HD 189733 b, for which atmospheric water has been detected with a model mixing ratio of 5×10^{-4} (Tinetti et al. 2007), as our test case: orbital and physical parameters for the host star and the planet were obtained from the Extrasolar Planets Encyclopaedia (www.exoplanet.eu). If we consider an atmospheric shell analogous in size to the Jovian stratosphere, i.e. about 300 km and with a average density of 2×10^{-8} g cm^{-3} (from the geometric mean of the extreme values reported by Young et al. 2005 for the Jovian stratosphere), the water content of this shell would be about 2.5×10^{17} g.

As possible impactors, we consider a population of star-grazing exocomets modelled after the 1265 Sun-grazing comets observed by SOHO since 1996: their orbital parameters were obtained from the JPL Small Bodies Database Search Engine (http://ssd.jpl.nasa.gov/sbdb_query.cgi). Sun-grazing comets observed by SOHO have high orbital inclination values (i.e. ~140°) therefore our preliminary estimate gives 1 impact on our test planet every 200 years. Assuming an ecliptic population of star-grazing exocomets, our preliminary estimate gives the larger flux of 1 impact every 20 years. The 100

comets for which we have estimates of the diameter range in size between 0.5 km to 60 km. If we consider the whole sample, the average diameter is about 5 km, i.e. the estimated size of comet Shoemaker-Levy 9, while if we ignore comets larger than 10 km, to compensate for the observational bias favouring larger objects respect to smaller ones, the average diameter is about 3 km. We will consider this value as the reference one.

Assuming a density of 1 g cm^{-3}, the mass of these bodies would range between $5x10^{14}$ g (1 km) and $6.5x10^{16}$ g (5 km), with our reference case (3 km) being $1.4x10^{16}$ g. From Mumma & Charnley (2011), we can assume an average water content of 72.8% of their mass. Therefore, each of these impactors would bring, on average, $1x10^{16}$ g. This implies that it would take the cumulative water budget of about 25 cometary impacts to reproduce the water content of the atmospheric shell we considered. Equivalently, the water content delivered by cometary impactors should be able to survive in said shell between $5x10^{2}$ years (1 impact every 20 years) and $5x10^{3}$ years (1 impact every 200 years). The values obviously assume that all the cometary water is released in the stratosphere of the exoplanet, which is not necessarily the case. Note that also this toy model should be regarded just as a more sophisticated back-of-the-envelope calculation, as the uncertainties on both the observational constrains and the assumptions can plausibly affect the order of magnitude of the values here considered.

As an example of the uncertainties affecting these estimates, Tinetti et al. (2007) report that changing the mixing ratio of water in the atmosphere of HD 189733 b by plus or minus one order of magnitude does not significantly affect the fit to the observational data. This uncertainty on the mixing ratio has significant implications for the time required to accumulate the expected water content. In the most favourable case, it would take only a couple of impacts to provide the required water budget or, alternatively, water would need to survive in the atmospheric shell only about 50 years (consider that water from the Shoemaker-Levy 9 impact resided in the Jovian stratosphere for at least 14 years at the time of the observations used by Cavalié et al. 2013). In the most unfavourable case, cometary water would need about $5x10^{4}$ years to accumulate.

From an observational perspective, the effects of the secular contamination can be expressed in terms of the mixing ratio that cometary impactors would produce. From the previous calculations, we can derive the following empirical relationship for the mixing ratio produced by a cometary impactor in the stratosphere of an exogiant planet:

$$m_r = 2.98\times 10^{-6}\,\chi\left(\frac{D_{comet}}{1\,km}\right)\left(\frac{\rho_{atmosph.}}{2\times 10^{-5}\,kg\,m^{-3}}\right)^{-1}\left(\frac{\Delta R}{100\,km}\right)^{-1}$$

where m_r is the mixing ratio of atmospheric water contributed by the impactor, χ is the fraction of the impactor dissolved in the considered atmospheric shell (i.e. the effective amount of water delivered in the observable region) and ΔR is the thickness of the atmospheric shell considered. This relationship can be used to obtain a rough estimate of the effects of cometary impactors for what it concerns water, but similar relationships can be derived for other high-Z elements and populations of impactors.

Processes affecting atmospheric composition after cometary impacts

Each fragment of the impactor can reach a different depth inside the planet. The basic properties of the impacts of SL9 were presented by Chevalier & Sarazin (1994 ApJ, 429, 863). A larger impactor

reaches deeper inside the planet. In the case of SL9 fragments the maximum depth corresponds approximatively to 500 km (about 1kbar). At this depth the fragments explode and liberate all their energy. In a timescale of 1 second the hot gases generated by the explosion rises in the higher parts of the atmosphere characterized by lower opacities, where they can have a luminosity of the order of 1025 erg/s in the near infrared. The shocked material can reach temperatures between 4000-5000 K, in these conditions there is the possibility to form new chemical species from the atmospheric material, as in the case of H_2S detected in the atmosphere of Jupiter only after the impact of SL9 fragments. Convective motions in the upper part of the atmosphere, and atmospheric circulation, provide a rapid mixing of the newly formed species in short time scales (few days) in the planetary atmosphere.

The previous results rely on the assumption that the planet is fully convective. However if a radiative zone is present in the planet, that separates the upper convective atmosphere and the metallic interior, the results of an impact can be different and can affect the chemical composition of the planet for longer timescales. If the impactor is so large that it explodes below the radiative zone, the rising bubbles of gas act as a dredge, in a similar way to the well-known effect of dredge-up in AGB stars. In this case the He-rich material below the radiative zone is brought to the surface, and the upper atmospheric material is depleted in heavier elements and chemical species.

Discriminating between the different effects

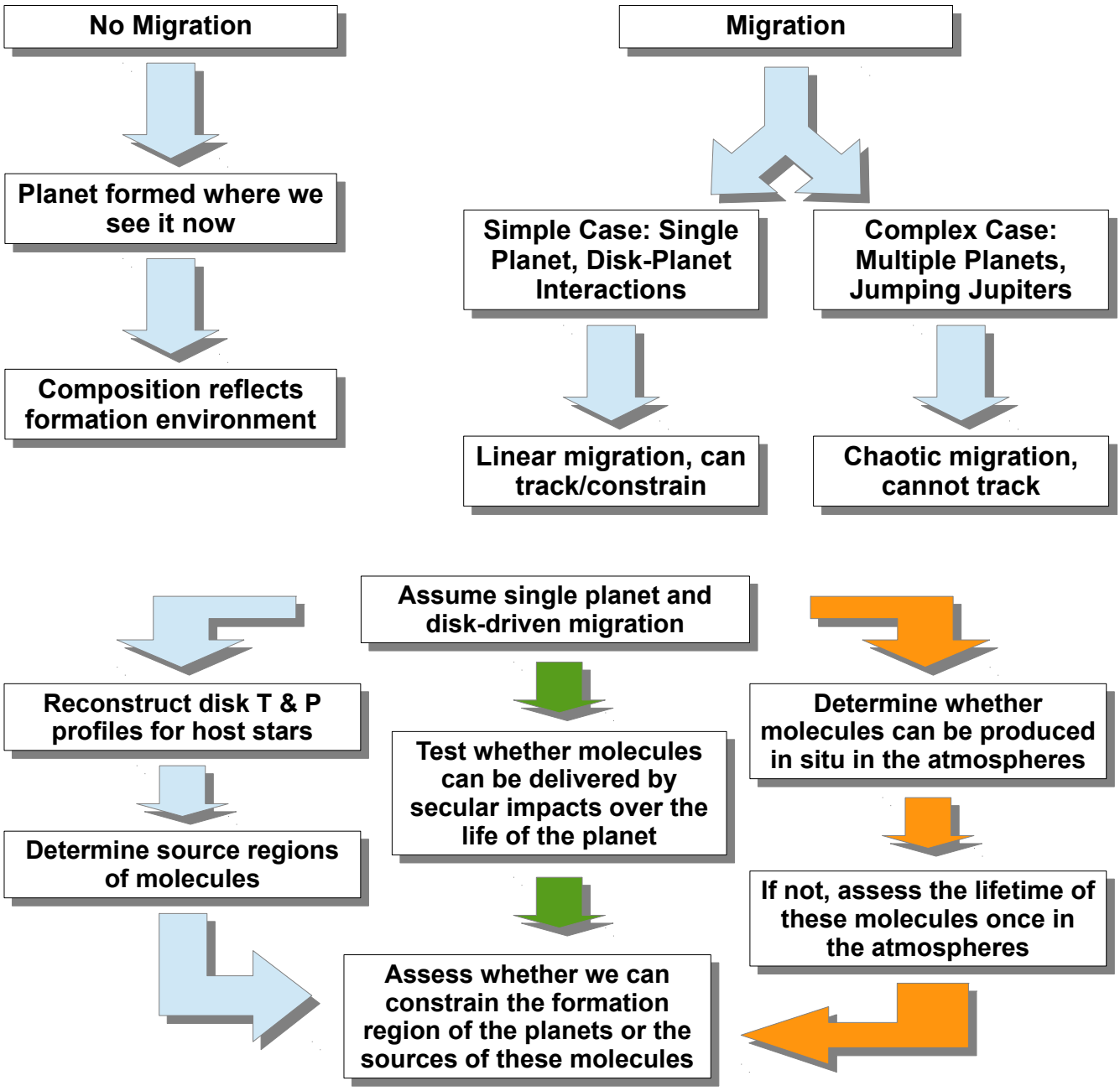

Bibliography

Adams, E.R., Seager, S., Elkins-Tanton, L., 2008, Ap.J., 673, 1160

Baruteau, C., Meru, F., Paardekooper, S.-J., 2011, MNRAS, 416, 1971

Bean, J.L., et al, 2011, Ap.J., 743, id. 92

Cavalié, T., et al. 2013. Astronomy & Astrophysics 553, id. A21.

Chambers J., E. 2009. Annual Review of Earth and Planetary Sciences 37, 321-344.

Chambers J. E., Wetherill G. W. 2001. Meteoritics and Planetary Science 36, 381-399.

Chatterjee, S., Ford, E.B., Matsumura, S., Rasio, F.A., 2008, Ap.J., 686, 580

Chevalier, Sarazin, 1994, Ap.J, 429, 863

Cook, A. F., Duxbury T. C. 1981. Journal of Geophysical Research 86, 8815-8817.

Coradini, A., Magni, G., Federico, C. 1981. Astronomy and Astrophysics 98, 173-185.

Coradini, A., Turrini, D., Federico, C., Magni, G. 2011. Space Science Reviews 163, 25-40.

D'Angelo G., Marzari F. 2012. The Astrophysical Journal 757, id. 50

Gomes R., Levison H.F., Tsiganis K., Morbidelli A. 2005. Nature 435, 466-469.

Guillot T., Gladman B. 2000. Disks, Planetesimals, and Planets, ASP Conference Proceedings, Vol. 219, edited by F. Garzón, C. Eiroa, D. de Winter, and T. J. Mahoney. Astronomical Society of the Pacific.

Hahn J. M., Malhotra R. 2005. The Astronomical Journal 130, 2392-2414.

Kley, W., Nelson, R.P., 2012, ARAA, 50, 211

Lewis J. S. 2004. Physics and Chemistry of the Solar System. London, UK; Elsevier Academic Press.

Lissauer, J., et al., 2011, Nature, 470, 53-58

Madhusudhan, N., et al. 2011, Nature, 469, 64

Madhusudhan, N., Seager, S., 2011, Ap. J., 729, 41

Marzari F., Weidenschilling S. J. 2002. Icarus 156, 570-579

Matter, A., Guillot, T., Morbidelli, A. 2009. Planetary and Space Science 57, 816-821

Mayor, M., et al, 2009, A & A, 507, 487-494

Morbidelli A., Levison H. F., Tsiganis K., Gomes R. 2005. Nature 435, 462-465.

Moses, J.I., et al., 2013, Ap.J., submitted

Mumma M. J., Charnley S. B. 2011. Annual Review of Astronomy and Astrophysics 49, 471-524.

O'Brien D. P., Morbidelli A., Bottke W. F. 2007. Icarus 191, 434-452.

Oberg, K., Murray-Clay, R., Bergin, E.A., 2011, Ap.J., 743, id. L15

Papaloizou J. C. B., et al. 2007. In: Protostars and Planets V, Eds. B. Reipurth, D. Jewitt, and K. Keil, Tucson, Arizona; University of Arizona Press.

Petit J., Morbidelli A., Chambers J. 2001. Icarus 153, 338-347.

Safronov, V. S. 1969. Evolution of the protoplanetary cloud and formation of the earth and planets.

Translated from Russian in 1972. Keter Publishing House, 212 pp.

Swain, M.R. et al. 2009, Ap.J. 704, 1616-1621

Taylor F. W. et al. 2004. In: Jupiter. The planet, satellites and magnetosphere. Edited by F. Bagenal, T. E. Dowling, W. B. McKinnon. Cambridge, UK; Cambridge University Press.

Tera F., Papanastassiou D. A.; Wasserburg G. J. 1974. Earth and Planetary Science Letters 22, 1

Tinetti, G. et al, 2007, Nature, 448, 169

Tsiganis K., Gomes R., Morbidelli A., Levison H. F. 2005. Nature 435, 459-461.

Turrini, D., Coradini, A., Magni, G. 2012. The Astrophysical Journal 750, id. 8.

Turrini, D., Magni, G., Coradini, A. 2011. MNRAS 413, 2439-2466.

Walsh K. J., Morbidelli A., Raymond S. N., O'Brien D. P., Mandell A. M., 2011. Nature 475, 206.

Walsh K. J., Morbidelli A., Raymond S. N., O'Brien D. P., Mandell A. M., 2012. M&PS 47, 1941.

Weidenschilling S. J. 2008, Physica Scripta 130, 014021.

Weidenschilling S. J., Marzari F. 1996, Nature 384, 619-621.

Weidenschilling, S. J. 1975. Icarus 26, 361-366.

Weidenschilling, S. J., Davis, D. R., Marzari, F. 2001. Earth, Planets, and Space 53, 1093-1097.

Wetherill G. W. 1992. Icarus 100, 307-325.

Young, L. A., Yelle, R. V., Young, R., Seiff, A., Kirk, D. B. 2005. Icarus 173, 185-199.

Zhu, Z., Hartmann, L., Nelson, R.P., Gammie, C.F., 2012, Ap.J., 746, id. 110